



**LETTER • OPEN ACCESS**

## Unraveling the dynamics of atmospheric methane: the impact of anthropogenic and natural emissions

To cite this article: Bo Fu *et al* 2024 *Environ. Res. Lett.* **19** 064001

View the [article online](#) for updates and enhancements.

You may also like

- [Evaluating the contribution of methanotrophy kinetics to uncertainty in the soil methane sink](#)

Hannah Dion-Kirschner, Newton H Nguyen, Christian Frankenberg *et al.*

- [The growing role of methane in anthropogenic climate change](#)

M Saunois, R B Jackson, P Bousquet *et al.*

- [A process-based model of methane consumption by upland soils](#)

A F Sabrekov, M V Glagolev, P K Alekseychik *et al.*

# ENVIRONMENTAL RESEARCH LETTERS



## OPEN ACCESS

RECEIVED  
22 February 2024

REVISED  
8 April 2024

ACCEPTED FOR PUBLICATION  
1 May 2024

PUBLISHED  
9 May 2024

## LETTER

# Unraveling the dynamics of atmospheric methane: the impact of anthropogenic and natural emissions

Bo Fu , Yongye Jiang, Guolong Chen, Mengmeng Lu, Yuqin Lai, Xinhao Suo and Bengang Li<sup>\*</sup>

College of Urban and Environmental Sciences, Institute of Carbon Neutrality, Peking University, Beijing 100871, People's Republic of China

\* Author to whom any correspondence should be addressed.

E-mail: [libengang@pku.edu.cn](mailto:libengang@pku.edu.cn)

**Keywords:** methane, climate change, anthropogenic, wetland

Supplementary material for this article is available [online](#)

Original content from this work may be used under the terms of the Creative Commons Attribution 4.0 licence.

Any further distribution of this work must maintain attribution to the author(s) and the title of the work, journal citation and DOI.



## Abstract

The reduction in methane concentration is crucial for achieving the goals of the Paris agreement. However, its annual growth rate is unstable, and understanding the reasons for changes in methane growth is essential for climate policy-making. Currently, there is considerable uncertainty regarding its attribution. Here, we utilize multi-source data and optimal fingerprinting methods to detect the contributions of several key drivers to the methane trend and interannual variability. We find that the methane growth trend is primarily influenced by anthropogenic emissions, while interannual variability is predominantly determined by wetland and biomass burning emissions. This result underscores the central role of anthropogenic emissions in methane dynamics, providing confidence in the effectiveness of human efforts to control methane atmospheric concentrations through emission reductions. It also helps alleviate concerns about the recent surge in atmospheric methane concentration, as it may be a short-term peak caused by increased wetland emissions rather than a long-term change.

## 1. Introduction

Methane ( $\text{CH}_4$ ), the second largest greenhouse gas, has more than doubled its atmospheric concentration relative to pre-industrial levels and contributes to a radiative forcing of  $0.43\text{--}0.65 \text{ W m}^{-2}$  [1]. The current atmospheric concentration surpasses levels aligned with the Paris agreement goals, underscoring the urgency of reducing methane to limit global warming to 1.5 and 2 degrees Celsius [2–5]. Currently, global efforts to mitigate  $\text{CH}_4$  are gaining traction, with countries progressively committing to reducing methane emissions through the Global Methane Pledge and national action plans [6].

The observational atmospheric methane growth has varied over the past few decades. In retrospect, growth, stagnation, and growth trends have been observed since the 1980s [7]. The differences of methane growth within different phases is very large and leads to contradictory explanations [2, 8]. Moreover, the urgent need for an explanation of methane concentration variability is heightened by the consecutive record-breaking annual increases observed since the

2020s [9, 10]. Only through a comprehensive understanding of past variations can efforts be targeted to reduce atmospheric  $\text{CH}_4$  concentrations [11].

The attribution of annual methane growth in the atmosphere is a topic of considerable interest [10, 12–14]. This growth is determined by the imbalance between sources and sinks, both of which exhibit significant uncertainties [15]. Anthropogenic methane emission, hydroxyl radical ( $\text{OH}$ ), wetland methane emission, and biomass burning emission are the main drivers of atmospheric methane change. Anthropogenic emissions of methane are regarded as the major contributor to the rise in atmospheric methane in several studies [13, 14], which come primarily from agriculture, fossil fuel production and use, and waste disposal. Wetland emissions are the major natural methane source [15], which is sensitive to climate and have large interannual variabilities [16, 17]. Biomass combustion emissions are also closely linked to climate and have a large interannual variability, although their contribution to atmospheric methane is moderate [18]. Hydroxyl radical dominates atmospheric methane sinks. Due to the too short

lifetime of OH, the trend of OH and methane lifetime are obtained based on atmospheric chemical models (e.g [19]). or methyl chloroform (e.g [20]).

In this study, we decomposed the atmospheric methane growth into trends and interannual variabilities, and evaluated the roles of these four drivers. Utilizing a box model called OSCAR [21], we simulated methane growth using external driver data. These external datasets encompassed the four drivers—three anthropogenic methane emission datasets, six OH concentration datasets, four wetland emission datasets, and one biomass burning dataset—which were employed to drive the OSCAR model. This resulted in a comprehensive ensemble of 72 members ( $3 \times 6 \times 4 \times 1$ ), constituting in a ‘meta-simulation’ (please refer to supplementary table 1). Based on multiple data sources in the meta-simulation can mitigate the impact of data uncertainty on the results. Furthermore, we introduced the optimal fingerprint method [22] to detect the contributions of the four drivers to methane trends and variability. Although widely employed in attribution research (e.g. [23–25]), this approach may be novel in the context of methane attribution. Through this methodology, we can provide quantitative insights into the statistical significance of each driver’s contribution.

## 2. Assessing model performance in annual atmospheric methane growth

The meta-simulation (72 members) was conducted to model the growth of atmospheric methane from 1984 to 2018. Each simulation member was driven by distinct combinations of datasets, and their differences arose from variations in the driver datasets. A comparison of the ensemble results with the observed annual growth shows that our model simulations accurately capture both the trend and variability of the change of atmospheric methane (figure 1(a)). The simple model average and Bayesian model average of the simulations align well with the observed growth rate, effectively capturing the decline observed between 1984 and 2006, the subsequent rise from 2007 to 2018, and even reproducing some of the peaks and valleys in the growth patterns (figure 1(a)).

The Taylor plot (figure 1(b)) provides a visual comparison between simulated and observed results in terms of the root mean square error (RMSE) and correlation coefficients. This plot quantitatively measures the accuracy of the simulated outcomes. Concerning the annual growth rates of methane, the majority of simulations exhibit RMSE values ranges 2.3–6.8 ppb, equivalent to 0.5–1.5 standard deviation of the observed values. The simple model average and Bayesian model average demonstrate smaller RMSE values of 3.5 and 3.0 ppb, respectively. The indication of the generally high accuracy of the model simulations relative to observations lays the foundation for

exploring the drivers behind methane concentration growth.

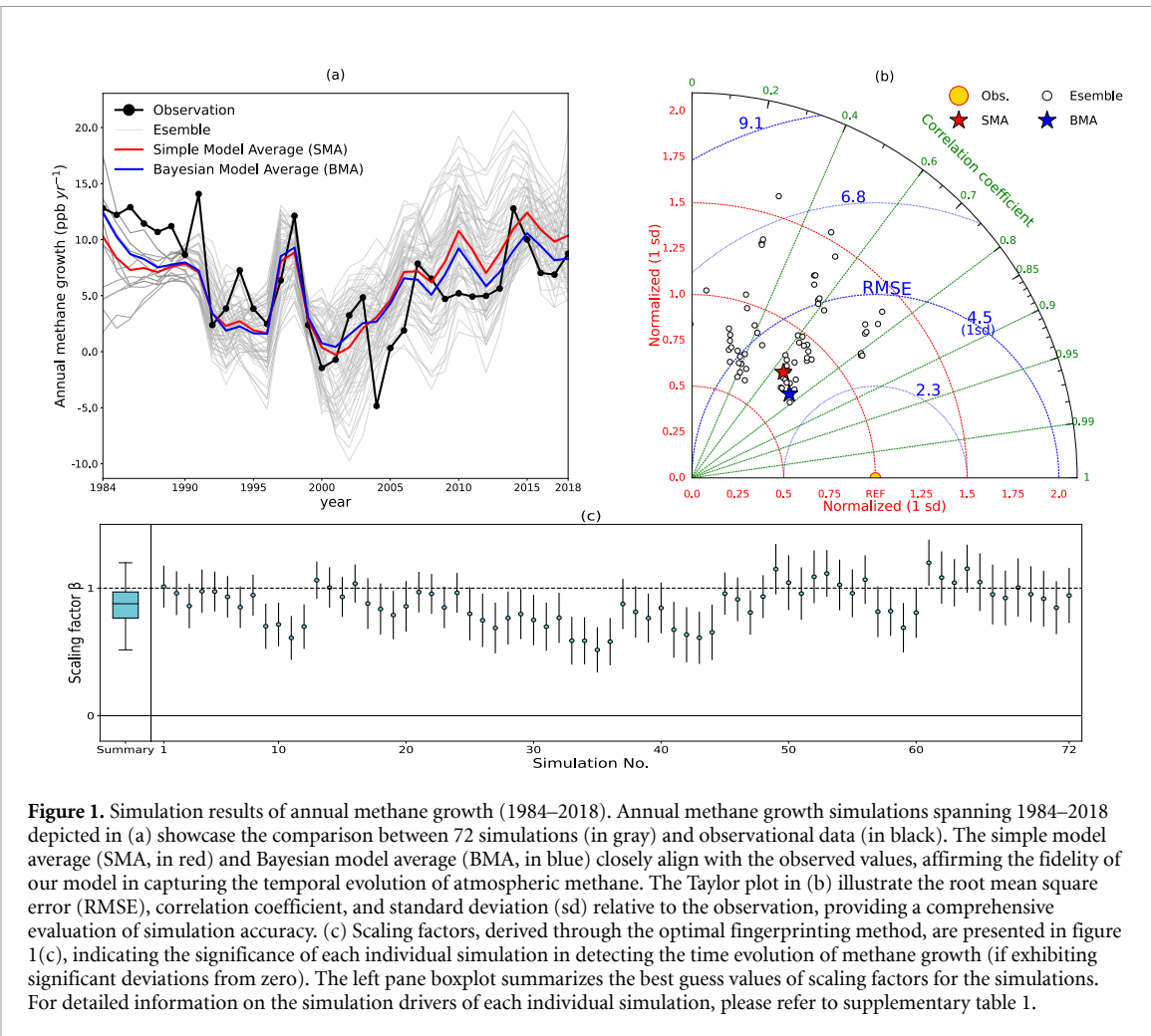
We utilized a one-way optimal fingerprinting method to assess the ability of each ensemble member to capture the methane growth trend. The significant differences in the scaling factors (regression coefficients)  $\beta$  from zero indicate the capability of the model to capture the changes in methane growth. Additionally, if the confidence interval of the scaling factor covers one, it signifies consistency between the simulated and observed variability. As illustrated in figure 1(c), all 72 simulations demonstrated scaling factors that were significantly different from zero, with many close to one. This implies a clear detection and successful attribution of the contributions to methane growth forced by all drivers. Based on this, in the subsequent sections, we explore the individual contributions of anthropogenic emissions, wetland emissions, biomass burning emissions, and OH concentrations to both the trend and variability observed in methane growth.

## 3. Attributing the trend and variability in methane growth

Given that the trends and variability in methane concentration growth might be driven by different factors, we decompose it into two components: trends and variability. Trends were derived using three methods: ensemble empirical mode decomposition (EEMD), moving average (MA), and piecewise linear function (PLF), while variability was obtained by subtracting the trend from the timeseries. The consistency among the three methods was high (supplementary figure 1). For brevity, we present only the results from the EEMD method in the main text (figure 2), with outcomes from the other two methods provided in extended data figure 1.

A consistent alignment between the trends and variability simulated by the modeled and observed data can be found. The trend of annual methane growth shows a sustained decreasing trend in the first half of the study period, followed by a gradual increase in the second half, indicating a slowdown followed by an acceleration in methane atmospheric concentration growth rate (figure 2(a)). In the initial years, the model tended to underestimate methane growth, which may be attributed to discrepancies in emission inventories. The consistency among the three emission inventories was relatively low in the early years but notably improved in later years (supplementary figure 2(a)). Overall, although there are substantial differences among the model-simulated members and initial underestimations, the trends simulated by the model align quite well with the observed trends (figure 2(b)).

Regarding interannual variability, the model performed well overall (figure 2(c)), notably in capturing some peaks and troughs, such as the growth peak



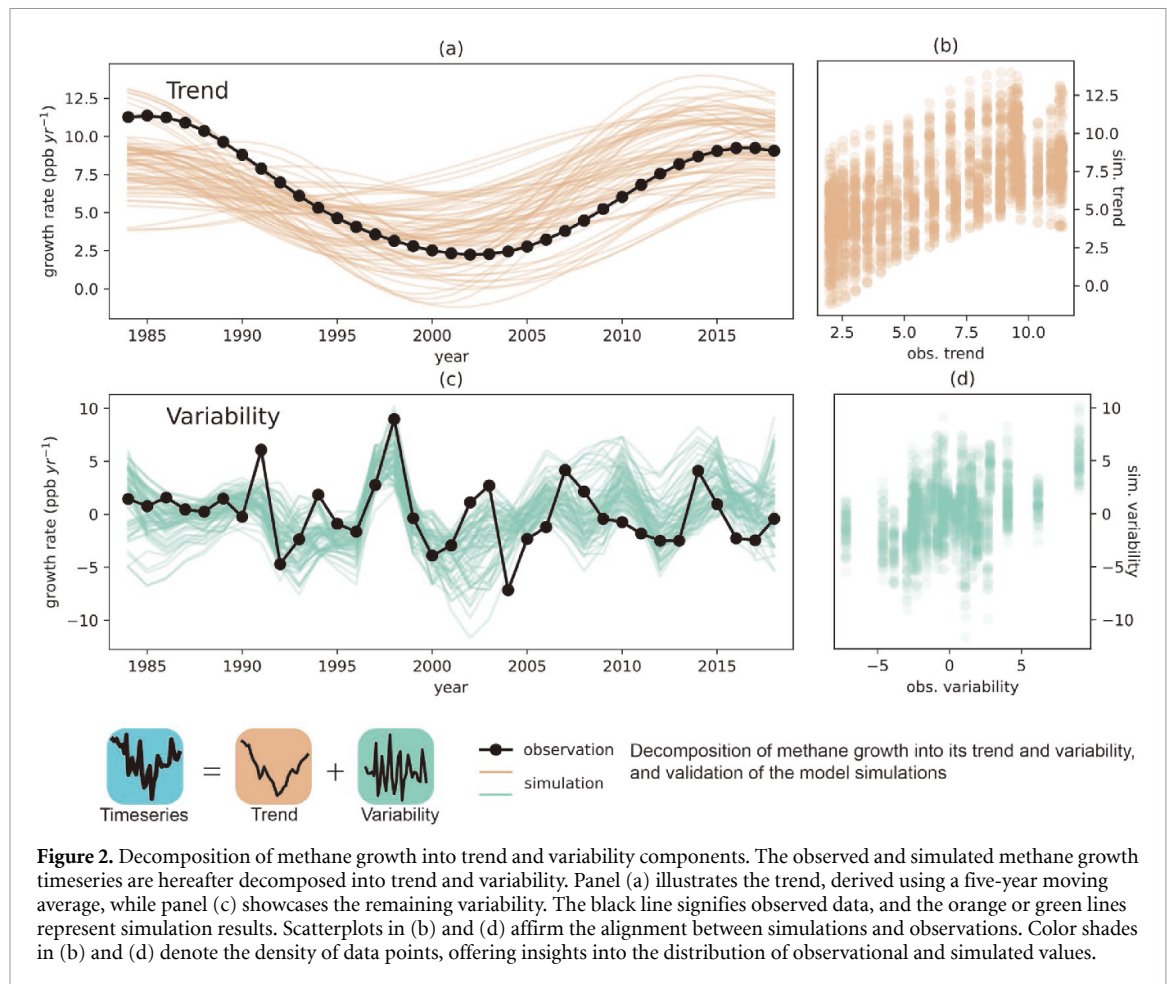
in 1998. This suggests that the driving datasets used in the model encompassed the factors influencing methane variability. Nevertheless, it is important to acknowledge that the model also generates peaks that are not observed, as seen in 2010, which could potentially result from biases within the driving data.

Additionally, based on the optimal fingerprinting method, the trends and variability of the methane concentration growth can be captured by the model (left-hand panel of figures 3(a) and (b)). The scaling factors for the trend range from 0.7 to 1.3, clustered around 1, indicating a relatively accurate modeling of the trend across simulations. In terms of variability, the scaling factors are concentrated between 0 and 1, indicating a significant capture of variability, yet also suggesting that the model simulations tend to overestimate variability.

Furthermore, we evaluated the contributions of anthropogenic emissions, hydroxyl radicals, wetland emissions, and biomass burning emissions to the trends and variability in methane growth. We conducted a series of controlled experiments, where only one factor drove the model in each experiment, while the other three factors remained at their multi-year averages. Subsequently, we utilized the optimal

fingerprinting method to regress the observed trends and variability of methane back to the simulated trends and variability from the controlled experiments, thereby assessing the impact of each driver factor.

For trend regression, most simulations agreed on positive scaling factors for anthropogenic methane emissions, whereas the scaling factors for other drivers were not significantly different from zero according to T-tests and binomial tests at a 95% confidence level. This indicates that the trends in methane growth rate are primarily influenced by anthropogenic emissions (see figure 3(a), extended data figures 2(a), and 3(a)). Supplementary figure 3 presents a juxtaposition analysis of the trends in anthropogenic emissions and methane growth rates. It shows that a period of stability in anthropogenic emissions coincides with a decline in the methane growth rate, suggesting a gradually approach towards equilibrium. Conversely, an increase in anthropogenic emissions is associated with a rise in the methane growth rate. However, it is important to note that in the early part of the study period, the trends indicated by EDGAR diverge from those shown by CEDS and GAINS.



In terms of variability regression, the scaling factors for anthropogenic methane emissions displayed signs of uncertainty, suggesting that anthropogenic emissions do not determine the variability in methane growth. Conversely, the scaling factors for wetland emissions and biomass burning consistently remained above zero, indicating their detected contribution to variability (see figure 3(b), extended data figures 2(b) and 3(b)). Comparing the scaling factors of the individual factors with those from the full-factor simulations, it appears that wetland emissions play a more crucial role in the variability of methane growth than biomass emissions. OH contributions were not consistently detected on both trends and variability. To summarize, trends in methane growth are predominantly driven by anthropogenic emissions, whereas variability is jointly influenced by wetland and biomass emissions.

#### 4. Conclusion and discussion

Methane growth is an important and multifaceted issue, primarily driven by anthropogenic emissions, wetland emissions, biomass emissions, and OH concentrations. However, each process entails significant uncertainties, making attribution of methane growth trends a challenging task. In this study, we address

this issue by conducting a meta-simulation driven by multiple source datasets (including 3 anthropogenic inventories, 6 OH concentration datasets, 4 wetland inventories, and 1 biomass burning inventory), forming a 72-member ensemble. Each individual simulation is treated as a distinct probability, allowing for probabilistic attribution analysis. Through this methodological design, we aim to enhance confidence in our attribution results regarding methane growth.

The multi-dataset driven simulation is designed to reflect the inherent uncertainties throughout the process as much as possible. For instance, the six OH datasets originate from diverse sources: three from 3D chemical simulations, two from box model simulations, and one from the CH<sub>3</sub>CCl<sub>3</sub> proxy. Although they generally exhibit an increasing trend during the study period, the variability among them is notably pronounced, especially between the CH<sub>3</sub>CCl<sub>3</sub> proxy and others driven by NO<sub>x</sub> emissions (see supplementary figure 2(b)). The performance of the driver datasets in capturing the methane growth and one-way optimal fingerprinting method are also different as shown in supplementary figure 4. Although we have endeavored to collect a diverse driving data, the limitations in the datasets are still evident. For example, the coverage years of different datasets are limited, wetland emission datasets are entirely based

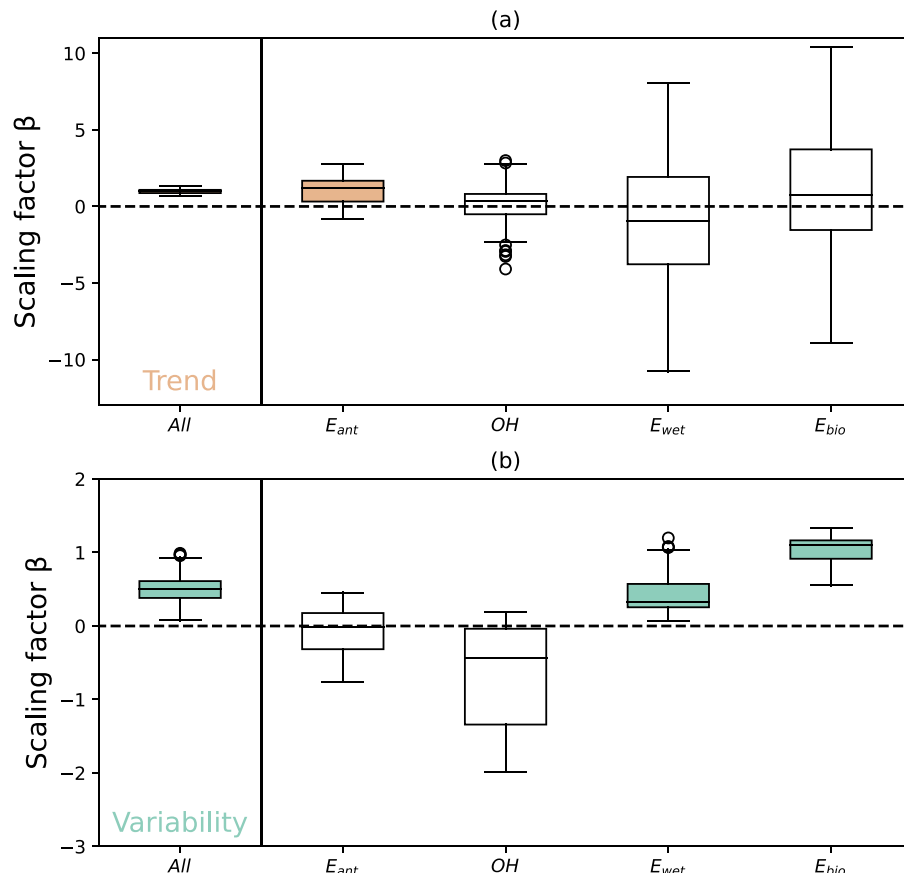


**Figure 3.** Scaling factors for trend and variability of methane growth. The trend and variability of methane growth are derived with EEMD. The results derived from MA and PLF can be found in extended data figures 2 and 3. In panel (a), scaling factors based on one-way regression (left) and four-way regression (right) are presented for the trend of methane growth. The left side of the panel displays scaling factors for all drivers, validating that the trend can be effectively captured by simulations. On the right side of the panel, scaling factors for anthropogenic methane emission ( $E_A$ ), hydroxyl radical (OH), wetland methane emission ( $E_W$ ), and biomass burning emission ( $E_B$ ) are shown. A filled boxplot indicates that the respective driver significantly contributes to the trend. (Significance is determined at a 95% confidence level through T-tests and binomial tests, confirming that the scaling factors are greater than zero). Panel (b) is the same, but attributes the variability of methane growth to the drivers.

on models with a lack of observational data, and there is only a single source for biomass burning datasets used in this study. To better attribute methane growth, the development of both observational and model data is imperative.

In line with previous studies [13, 14], we also affirmed that anthropogenic methane emissions constitute the primary determinant of the growth trend in methane levels. Consequently, the reduction of anthropogenic emissions is considered an effective measure for altering atmospheric methane growth trends. Currently, commitments and actions aimed at reducing methane emissions are gradually emerging. This is evidenced by the global methane pledge during COP26 and the recent announcement of China's national methane emission control action plan [6]. These emission reduction commitments foreshadow a significant decrease in anthropogenic methane emissions in the near future. Therefore, we can anticipate a change in the atmospheric methane growth trend, and possibly even a reversal towards a declining trend. Our results underscore the critical role of anthropogenic emissions in shaping the trajectory of

atmospheric methane, as also highlighted in previous studies [13, 14, 26–28].

Our findings also reinforce the significant impact of nature emissions on the variability of methane growth. Bousquet *et al* [12] have previously highlighted the predominant influence of wetland emissions on the interannual variability in methane growth during the period from 1984 to 2003. Our research aligns with this assertion using different methodology and extends the timeframe, demonstrating that this conclusion remains robust even as methane concentrations continue to rise in the current decade. We attributed some historical positive peaks in the variability of methane growth to wetland emissions. The concerned surge in atmospheric methane is also explained by wetland emissions in recent studies [17, 20]. It can be inferred that the variability in annual growth is determined by natural emissions and not by human activities. Wetland methane emissions are governed by meteorological conditions [29, 30]. Given the considerable interannual variability of meteorological factors and decadal oscillations, such as El Niño,

wetland emissions, which are historically elevated in certain years, are likely to revert to average or lower levels. Thus, in the absence of significant changes in the climate equilibrium, the impact of wetland emissions on methane growth will fluctuate with meteorological conditions.

Our conclusions have implications on the recent surges in methane growth. However, our meta-simulation in the main text does not encompass the post-2020 surge in methane, due to the year limitation of most driver datasets. This limitation poses a challenge in directly correlating our conclusions with the recent increases. If more datasets were available for a sufficient range of years, the conclusion would be much stronger and more convincing. Recent surges in methane growth might represent short-term peaks rather than a shift in trend, potentially resulting in a decrease in the methane growth rate in the upcoming years. If so, it is crucial to focus on trends shaped by anthropogenic emissions rather than on the rapid growth observed in recent years. Encouraging vigorous efforts to mitigate anthropogenic methane emissions remains imperative.

## 5. Method

### 5.1. Box model

To simulate the atmospheric methane growth and estimate the impact of anthropogenic methane emissions, wetland emissions, biomass burning emissions, and OH on the atmospheric methane growth, a box model named OSCAR (Gasser 2017) is used. External datasets of the four drivers are used to drive OSCAR model in this study.

The OSCAR model is a reduced complexity climate model including a methane module. The growth of atmospheric  $\text{CH}_4$  ( $\frac{d}{dt}\text{CH}_4$ ) is determined by its emissions and sink ( $S^{\text{CH}_4}$ ) following the mass-balance equation:

$$\alpha_{\text{atm}}^{\text{CH}_4} \frac{d}{dt} \text{CH}_4 = E_{\text{ant}}^{\text{CH}_4} + E_{\text{wet}}^{\text{CH}_4} + E_{\text{bio}}^{\text{CH}_4} - S^{\text{CH}_4}.$$

Methane sink is caused by four processes: tropospheric oxidation by OH, stratospheric oxidation, oxidation in dry soils, and oxidation in the oceanic boundary layer. Of these four mechanisms, OH oxidation is the most important. We used external OH to drive the model, and the other three removal processes are simulated using the model defaults.

### 5.2. Driver datasets

We integrated three anthropogenic methane emission datasets, six OH concentration datasets, four wetland emission datasets, and one biomass burning dataset, resulting in 72 simulations ( $3 \times 6 \times 4 \times 1$ ), constituting a meta-analysis. Our motivation for utilizing multiple datasets was to mitigate the influence

of uncertainty associated with the driving data on the assessment outcomes, thereby enhancing the credibility of our findings.

The three anthropogenic methane emission datasets used were CEDS v2021 [31], EDGAR v8.0 [32], and GAINSv4 [33]. Among the six OH concentration datasets, four were sourced from the literature [13, 20, 28, 34], while the remaining two OH concentration datasets were simulated by OSCAR using the observed methane concentration [9] and emission inventories of NOX, CO, and VOC. Specifically, CEDS v2021 [31] and EDGAR v6.1\_AP [35] were employed. Four wetland emission datasets were obtained from WetCHARTs [36] and [13, 17, 27]. The biomass burning dataset utilized was GFED [37], with OSCAR simulating biomass burning data to fill in missing years. The driver datasets are plotted in supplementary figure 2.

### 5.3. Decomposition into trend and variability

In this study, the methane timeseries are decomposed into trends and variability. Trends are derived using three different methods: EEMD, MA, and PLF. The results from method EEMD are presented in the main text, while the outcomes from methods MA and PLF are provided in the supplementary information. They are largely consistent (supplementary figure 1). The variabilities are derived by subtracting the trend from the timeseries.

EEMD is a data analysis method employed for decomposing signals or time series data into a finite number of intrinsic mode functions (IMFs) and a residue. Among these IMFs, the lower-order IMFs are identified as the components representing trends. Unlike conventional methods like Fourier analysis, EEMD demonstrates adaptability and proficiency in effectively handling nonlinear and non-stationary signals. In this study, EEMD has been implemented using the Python package PyEMD.

MA refers to utilizing the multi-year MA as the representation of trend. In this study, a five-year sliding window is employed for the MA. PLF is characterized by multiple linear segments, each possessing distinct slopes within different intervals. PLF is frequently employed as a tool in signal processing or data modeling to enhance understanding and depiction of data behaviors or trends. In this study, the implementation of PLF utilized the Python package pwlf.

### 5.4. Optimal fingerprint method

The optimal fingerprint method is a regression-based method, which has been widely used for detection of climate change and attribution. These approaches are based on multivariate linear regression and assume that observed changes stem from a linear combination of externally forced signals and internal variability [25].

In this study, an optimal fingerprint method was employed to discern the influence of various drivers on atmospheric growth. We assume that the observed trend and variabilities in methane growth can be attributed to anthropogenic methane emission, hydroxyl radical, wetland methane emission, and biomass burning emission.

We regressed the observed methane changes  $X^{\text{obs}}$  onto the simulated changes  $X_i^{\text{sim}}$  which were driven by all drivers or each driver. The regression equation took the form  $X^{\text{obs}} = \sum \beta_i X_i^{\text{sim}} + \varepsilon$  where  $\varepsilon$  represents the residual error. The contribution is detected if the scaling factor  $\beta_i$  was significantly different from zero. This method allowed us to systematically evaluate how the drivers influence the observed trend and variabilities of methane growth. The optimal fingerprint method is used on a one-way regression for all drivers ( $X^{\text{obs}} = \beta_{\text{all}} X_{\text{all}}^{\text{sim}} + \varepsilon$ ) and four-way regression for each drivers ( $X^{\text{obs}} = \beta_{\text{ant}} X_{\text{ant}}^{\text{sim}} + \beta_{\text{oh}} X_{\text{oh}}^{\text{sim}} + \beta_{\text{wet}} X_{\text{wet}}^{\text{sim}} + \beta_{\text{bio}} X_{\text{bio}}^{\text{sim}} + \varepsilon$ ).

### Data availability statement

The OSCAR model is available at <https://github.com/tgasser/OSCAR>.

The data that support the findings of this study are openly available at the following URL/DOI: <https://github.com/pkufubo/Scripts-for-ERL-117807>.

### Acknowledgment

This study is supported by the National Natural Science Foundation of China (Grant No. 42201515) and the National Key R&D Program of China (No. 2022YFF0802503). We acknowledge Mr. Zhiping Zhang from Peking University for providing assistance with the trend obtainment method.

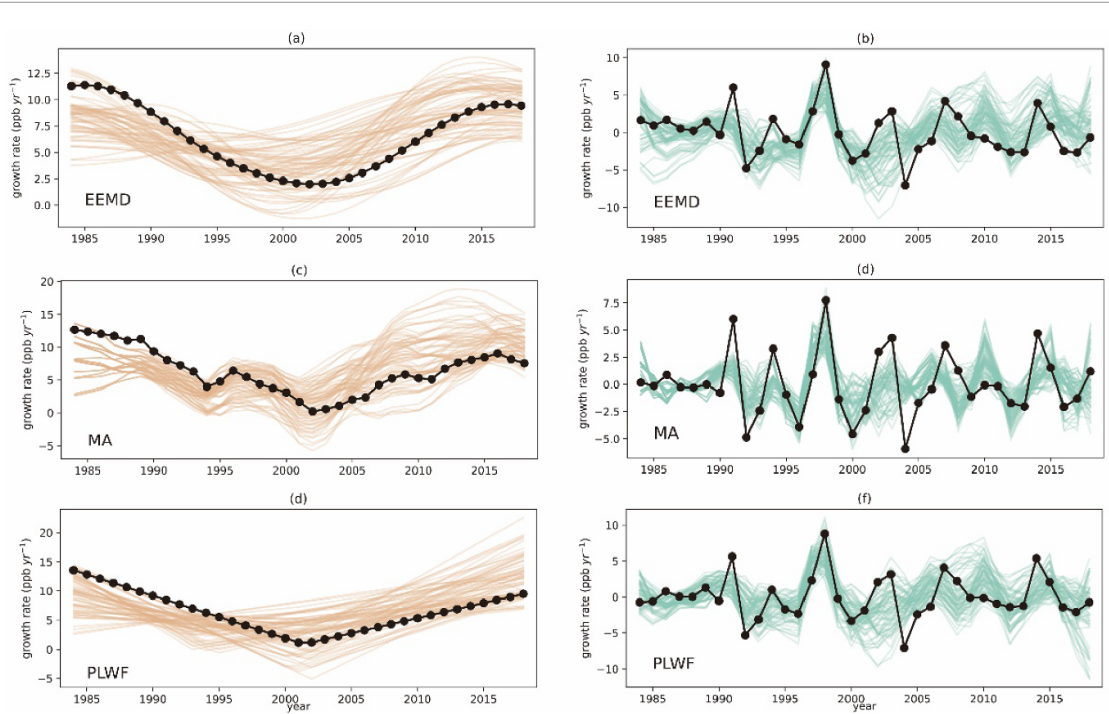
### Author contributions

B L and B F conceptualized the study. B F and Y J conducted all computational analyses. B F drafted the manuscript. X S, G C, Y L, and M L processed the input data and generated the visualizations. All co-authors contributed to editing the manuscript.

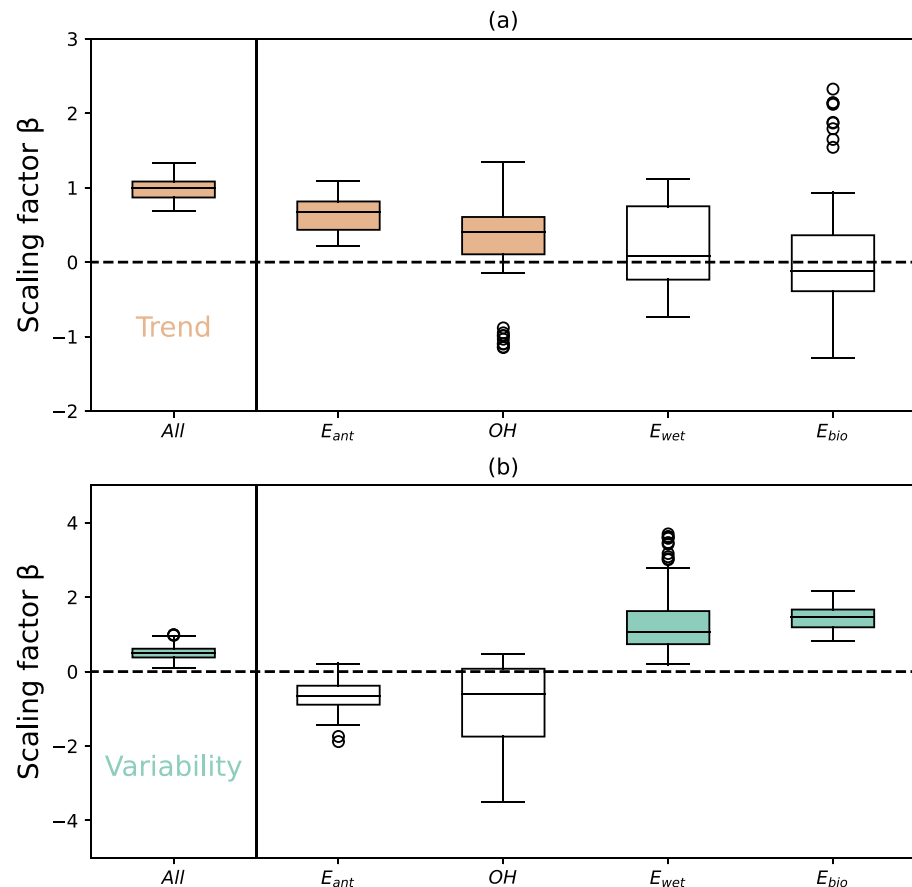
### Conflict of interest

The authors declare no competing interests.

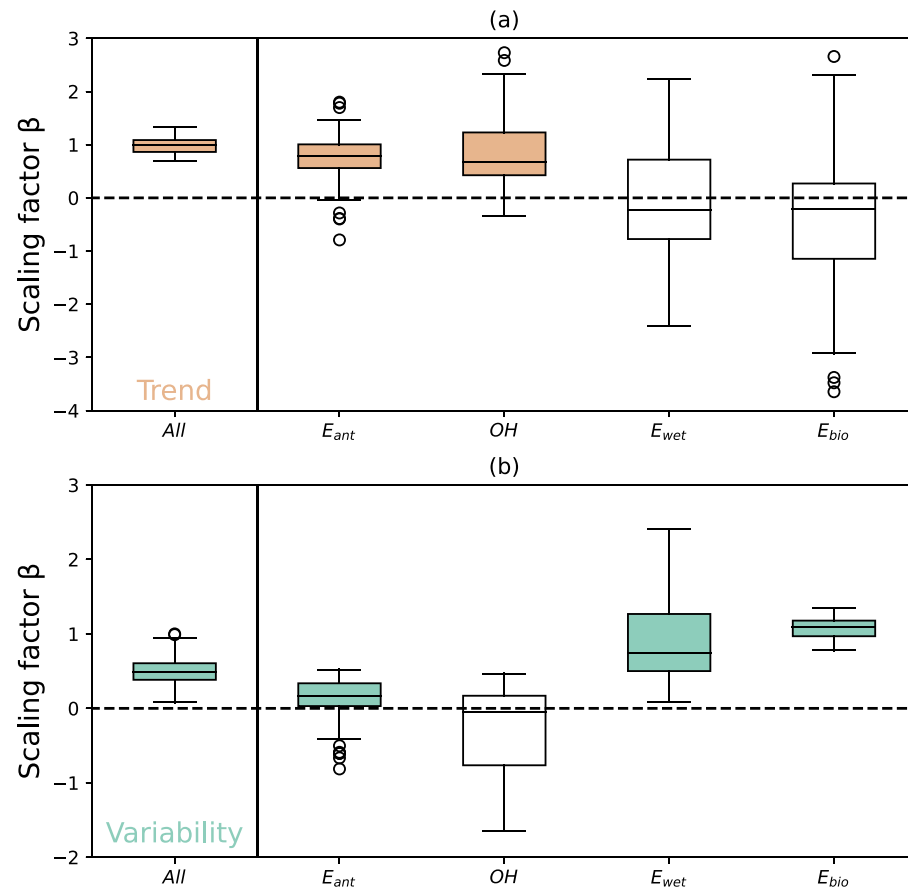
## Appendix



**Extended Data Figure 1.** Decomposition of methane growth with three method. Three method are used here to obtain the trend (a), (c), (d) and variability of methane growth (b), (e), (f). (a), (b) are derived with ensemble empirical mode decomposition (EEMD), which are the same as figures 2(a) and (c). (c), (d) are derived with moving average (MA). (e), (f) are derived with piecewise linear function (PLF).



**Extended Data Figure 2.** Scaling factors for trend and variability of methane growth. Same as figure 3, but the trend and variability of methane growth are derived with MA.



**Extended Data Figure 3.** Scaling factors for trend and variability of methane growth. Same as figure 3, but the trend and variability of methane growth are derived with PLF.

## ORCID iD

Bo Fu <https://orcid.org/0000-0003-1268-6348>

## References

- [1] IPCC 2021 Climate change 2021: the physical science basis ed V Masson-Delmotte *Contribution of Working Group I to the Sixth Assessment Report of the Intergovernmental Panel on Climate Change* (Cambridge University Press)
- [2] Nisbet E G et al 2019 Very strong atmospheric methane growth in the 4 years 2014–2017: implications for the Paris Agreement *Glob. Biogeochem. Cycles* **33** 318–42
- [3] Fletcher S E M and Schaefer H 2019 Rising methane: a new climate challenge *Science* **364** 932–3
- [4] Ganeshan A L et al 2019 Advancing scientific understanding of the global methane budget in support of the Paris Agreement *Glob. Biogeochem. Cycles* **33** 1475–512
- [5] Nisbet E G et al 2020 Methane mitigation: methods to reduce emissions, on the path to the Paris agreement *Rev. Geophys.* **58** e2019RG000675
- [6] Nisbet E G 2023 New hope for methane reduction *Science* **382** 1093–3
- [7] Nisbet E G, Dlugokencky E J and Bousquet P 2014 Methane on the rise—again *Science* **343** 493–5
- [8] Turner A J, Frankenberg C and Kort E A 2019 Interpreting contemporary trends in atmospheric methane *Proc. Natl Acad. Sci.* **116** 2805–13
- [9] Lan X, Thoning K W and Dlugokencky E J Trends in globally-averaged  $\text{CH}_4$ ,  $\text{N}_2\text{O}$ , and  $\text{SF}_6$  determined from NOAA global monitoring laboratory measurements Version 2023–11 (<https://doi.org/10.15138/P8XG-AA10>)
- [10] Peng S et al 2022 Wetland emission and atmospheric sink changes explain methane growth in 2020 *Nature* **612** 477–82
- [11] Wilson C 2023 Untangling variations in the global methane budget *Commun. Earth Environ.* **4** 318
- [12] Bousquet P et al 2006 Contribution of anthropogenic and natural sources to atmospheric methane variability *Nature* **443** 439–43
- [13] Skeie R B, Hodnebrog Ø and Myhre G 2023 Trends in atmospheric methane concentrations since 1990 were driven and modified by anthropogenic emissions *Commun. Earth Environ.* **4** 317
- [14] Zhang Z et al 2022 Anthropogenic emission is the main contributor to the rise of atmospheric methane during 1993–2017 *Natl Sci. Rev.* **9** nwab200
- [15] Saunois M et al 2020 The global methane budget 2000–2017 *Earth Syst. Sci. Data* **12** 1561–623
- [16] Zhang Z, Zimmermann N E, Stenke A, Li X, Hodson E L, Zhu G, Huang C and Poulet B 2017 Emerging role of wetland methane emissions in driving 21st century climate change *Proc. Natl Acad. Sci.* **114** 9647–52
- [17] Zhang Z, Poulet B, Feldman A F, Ying Q, Ciais P, Peng S and Li X 2023 Recent intensification of wetland methane feedback *Nat. Clim. Change* **13** 430–3
- [18] Worden J R, Bloom A A, Pandey S, Jiang Z, Worden H M, Walker T W, Houweling S and Röckmann T 2017 Reduced biomass burning emissions reconcile conflicting estimates of the post-2006 atmospheric methane budget *Nat. Commun.* **8** 2227
- [19] Zhao Y et al 2019 Inter-model comparison of global hydroxyl radical (OH) distributions and their impact on atmospheric methane over the 2000–2016 period *Atmos. Chem. Phys.* **19** 13701–23
- [20] Turner A J, Frankenberg C, Wennberg P O and Jacob D J 2017 Ambiguity in the causes for decadal trends in

- atmospheric methane and hydroxyl *Proc. Natl Acad. Sci.* **114** 5367–72
- [21] Gasser T *et al* 2017 The compact Earth system model OSCAR v2. 2: description and first results
- [22] Allen M R and Stott P A 2003 Estimating signal amplitudes in optimal fingerprinting, Part I: theory *Clim. Dyn.* **21** 477–91
- [23] Hegerl G C, Von Storch H A N, Hasselmann K, Santer B D, Cubasch U and Jones P D 1996 Detecting greenhouse-gas-induced climate change with an optimal fingerprint method *J. Clim.* **9** 2281–306
- [24] Min S K, Zhang X, Zwiers F W and Hegerl G C 2011 Human contribution to more-intense precipitation extremes *Nature* **470** 378–81
- [25] Hegerl G, Luterbacher J, González-Rouco F, Tett S F B, Crowley T and Xoplaki E 2011 Influence of human and natural forcing on European seasonal temperatures *Nat. Geosci.* **4** 99–103
- [26] Jackson R B, Saunois M, Bousquet P, Canadell J G, Poulter B, Stavert A R, Bergamaschi P, Niwa Y, Segers A and Tsuruta A 2020 Increasing anthropogenic methane emissions arise equally from agricultural and fossil fuel sources *Environ. Res. Lett.* **15** 071002
- [27] Chandra N *et al* 2021 Emissions from the oil and gas sectors, coal mining and ruminant farming drive methane growth over the past three decades *J. Meteorol. Soc. Jpn. II* **99** 309–37
- [28] He J, Naik V, Horowitz L W, Dlugokencky E and Thoning K 2020 Investigation of the global methane budget over 1980–2017 using GFDL-AM4. 1 *Atmos. Chem. Phys.* **20** 805–27
- [29] Hodson E L, Poulter B, Zimmermann N E, Prigent C and Kaplan J O 2011 The El Niño–Southern oscillation and wetland methane interannual variability *Geophys. Res. Lett.* **38** 8
- [30] Zhu Q *et al* 2017 Interannual variation in methane emissions from tropical wetlands triggered by repeated El Niño–Southern oscillation *Glob. Change Biol.* **23** 4706–16
- [31] O'Rourke P R *et al* 2021 CEDS v-2021-02-05 emission data 1975–2019 (version Feb-05-2021) (Zenodo) (<https://doi.org/10.5281/zenodo.4509372>)
- [32] Crippa M *et al* 2023 GHG Emissions of All World Countries (Publications Office of the European Union) ([https://doi.org/10.2760/953322\\_JRC134504](https://doi.org/10.2760/953322_JRC134504))
- [33] Höglund-Isaksson L, Gómez-Sanabria A, Klimont Z, Rafaj P and Schöpp W 2020 Technical potentials and costs for reducing global anthropogenic methane emissions in the 2050 timeframe—results from the GAINS model *Environ. Res. Commun.* **2** 025004
- [34] Nicely J M, Canty T P, Manyin M, Oman L D, Salawitch R J, Steenrod S D, Strahan S E, Strode S A 2018 Changes in global tropospheric OH expected as a result of climate change over the last several decades *J. Geophys. Res. Atmos.* **123** 10774–95
- [35] EDGAR 2022 Global air pollutant emissions (available at: [https://edgar.jrc.ec.europa.eu/dataset\\_ap61](https://edgar.jrc.ec.europa.eu/dataset_ap61))
- [36] Bloom A A, Bowman K W, Lee M, Turner A J, Schroeder R, Worden J R, Weidner R, McDonald K C and Jacob D J 2017 A global wetland methane emissions and uncertainty dataset for atmospheric chemical transport models (WetCHARTs version 1.0) *Geosci. Model. Dev.* **10** 2141–56
- [37] GFED 2022 Global fire emissions database version 4.1 including small fire burned area (GFED4s) (available at: [www.geo.vu.nl/~gwerf/GFED/GFED4/tables/GFED4s\\_CH4.txt](http://www.geo.vu.nl/~gwerf/GFED/GFED4/tables/GFED4s_CH4.txt))